

## The crystal structure of $3T$ muscovite

By NECIP GÜVEN and CHARLES W. BURNHAM\*

Geophysical Laboratory, Carnegie Institution of Washington  
Washington, D.C.

*Dedicated to Prof. Dr. G. Menzer on the occasion of his 70th birthday*

(Received April 14, 1967)

### Auszug

Die Kristallstruktur eines trigonalen Dreischicht-Muskowits ( $3T$ ) von Sultan Basin, Washington, wurde bestimmt und mittels Ausgleichsrechnung dreidimensional verfeinert. Die Raumgruppe ist  $P3_112$  ( $P3_212$ ). Die Gitterkonstanten sind:  $a = 5,1963 \pm 0,0004 \text{ \AA}$ ,  $c = 29,9705 \pm 0,0016 \text{ \AA}$ . Der Vergleich der Strukturdaten des  $3T$ -Muskowits mit denen eines üblichen  $2M_1$ -Muskowits zeigt, daß die Kationen im  $3T$  sowohl in tetraedrischen als auch in oktaedrischen Lagen partiell geordnet sind, während beim  $2M_1$  die Verteilung der Si und Al in tetraedrischen Lagen vollkommen ungeordnet ist, und daß die Struktur beim  $3T$  etwas weniger gewellt ist als beim  $2M_1$ -Muskowit. Die einzelne Glimmerschicht des  $3T$ -Muskowits hat die Raumgruppe  $C2$ , wogegen die Raumgruppe der entsprechenden Schicht des  $2M_1$ -Muskowits  $C\bar{1}$  ist; demnach sind die Schichten der beiden Muskowite nicht equivalent. In Anbetracht dieser Differenz wird die Ansicht geäußert, daß die beiden Muskowitformen nicht als Polytype, sondern als polymorphe Formen aus voneinander ableitbaren einzelnen Schichten zu bezeichnen sind.

### Abstract

The crystal structure of a natural sample of three-layer trigonal ( $3T$ ) muscovite from Sultan Basin, Snohomish County, Washington, has been determined and refined by least-squares methods using single-crystal counter intensity data. This specimen is trigonal, space group  $P3_112$  (or  $P3_212$ ) and has the following cell dimensions:  $a = 5.1963 \pm 0.0004 \text{ \AA}$ ,  $c = 29.9705 \pm 0.0016 \text{ \AA}$ . Comparison of  $3T$  muscovite structural parameters with those of the common  $2M_1$  muscovite shows that (a) cations are distributed in a partially ordered arrangement in both tetrahedral and octahedral sites in  $3T$ , whereas in  $2M_1$  the distribution of Si and Al in tetrahedral sites is completely disordered, and (b) the  $3T$  structure is slightly less corrugated than that of  $2M_1$  muscovite. The single mica layer of  $3T$  muscovite has space group  $C2$ , whereas the corresponding layer of  $2M_1$  muscovite

\* Present address: Department of Geological Sciences, Harvard University, Cambridge, Massachusetts.

has space group  $C\bar{1}$ ; hence these layers are not equivalent. Considering these differences, it is suggested that these forms of muscovite not be termed polytypes but rather polymorphs with derivative single layers.

### Introduction

Polymorphism of micas has remained a subject to prime interest to petrologists and clay mineralogists ever since HENDRICKS and JEFFERSON (1939) showed that these minerals crystallize with one of several layered structures, all of which are based on the same substructure. The substructure is a single mica layer about 10 Å thick consisting of two layers of tetrahedra (containing Si plus Al or Fe<sup>+3</sup>) separated by an octahedral layer (containing primarily Al or Fe<sup>+3</sup> in dioctahedral micas). In the idealized muscovite structure proposed by JACKSON and WEST (1930) the mica layer as a unit has monoclinic symmetry, while its surface layers of oxygen atoms form a hexagonal array. Hence, according to SMITH and YODER (1956), packing of the surface layers will be invariant with layer rotations of 60° or multiples thereof, and structures with different overall symmetry will result from varying the stacking sequence of individual mica layers.

It is clear that an ordered mica crystal can form only if structural control over the layer stacking sequence exists during growth. SMITH and YODER (1956) showed that only six distinct mica structures can be generated by stacking layers with a constant interlayer stacking angle. By treating mica structures as close-packed arrangements of anions, ZVYAGIN (1962) defines the possible structures in terms of the relative displacements of tetrahedral layers with respect to each other within the mica unit. Rather than considering the various structures as sequences of mica layers rotated with respect to each other as SMITH and YODER (1956) have done, ZVYAGIN (1962) preferred to think of them as a sequence of superpositions of composite layers having differing relative displacements of tetrahedral layers. In terms of stacking-sequence descriptions, there is clearly no real difference between the two methods. ZVYAGIN's approach, however, seems more desirable if one is attempting to relate structure type to growth mechanism, since he implies that stacking sequences result from growth "decisions" relating the position of one tetrahedral layer relative to another within each composite mica layer. We shall disregard any genetic implications and use SMITH and YODER's technique to describe different stacking modifications because of its geometric simplicity.

Recently Ross *et al.* (1966) determined the space groups and idealized cell geometry of the 36 possible structures having four or fewer layers in the repeat unit, and interlayer stacking angles of any combination of  $0^\circ$ ,  $\pm 60^\circ$ ,  $\pm 120^\circ$ , and  $180^\circ$ . These authors found that biotites (trioctahedral) are capable of forming any one of several structures with stacking sequences having combinations of  $0^\circ$  and  $\pm 120^\circ$  interlayer stacking angles. Dioctahedral muscovite, on the other hand, most commonly crystallizes with the  $2M_1$  structure (alternating  $+$  and  $-120^\circ$  interlayer stacking angles) and rarely with the  $3T$  structure (constant  $+120^\circ$  interlayer stacking angles). The  $1M$  structure ( $0^\circ$  rotation between layers) has been synthesized and compared with similar natural materials by YODER and EUGSTER (1955). VELDE (1965) suggested that  $1M$  is a metastable phase of muscovite. The absence of interlayer stacking angles of  $\pm 60^\circ$  and  $180^\circ$  in all micas except those containing Li is generally attributed to the reduction of symmetry of surface oxygen atoms from hexagonal in the ideal structure to trigonal (or pseudotrigonal) in those structures that have recently been determined (STEINFINK, 1962; BURNHAM and RADOSLOVICH, 1964; TAKÉUCHI, 1966).

The crystal structure of  $2M_1$  muscovite having the composition  $(K_{.94}Na_{.06})(Al_{1.84}Fe^{+3}_{.12}Mg_{.06})(Si_{3.11}Al_{.89})O_{10}(OH)_2$  was refined by RADOSLOVICH (1960) using Fourier methods to  $R = 17\%$  for all measured reflections, and again with the same film data, using least-squares methods by GATINEAU (1963) to  $R = 8\%$ . On the basis of mean bond lengths, RADOSLOVICH suggested that Al is preferentially located in one of the two crystallographically independent tetrahedral cation sites; GATINEAU's refinement indicated, on the other hand, little ordering of tetrahedral Al. GÜVEN (1967) has refined the structure of a  $2M_1$  muscovite in which he demonstrated complete lack of long-range order of tetrahedral Al. Until now no structural studies of either the  $1M$  or  $3T$  muscovite structures have been reported.

Although we now have considerable knowledge of the details of the  $2M_1$  structure, the reasons for the preference of muscovite for this structure, rather than one or more of the several possibilities, are not at all clear. RADOSLOVICH (1960) suggested that  $2M_1$  stability is related to the fact that interlayer K is not in the center of its coordination polyhedron, whereas TAKÉUCHI (1966) pointed out that structural control may be related to the direction of O—H bonds in the octahedral layers. Implicit in most discussions of this problem is the concept that the only difference between the various structures

is the stacking sequence, and hence that modifications of micas having identical compositions are *polytypes* with identical single layers. The concept of *polytypism*, as routinely applied to micas in the literature, requires the assumption of equivalence of the single mica layers—an assumption that, in the case of muscovite, is not justified on the basis of the structural knowledge to be presented below.

We report here a determination of the crystal structure of  $3T$  muscovite that we undertook with the problems stated above in mind. Specifically, we wanted to determine whether or not the single mica layer of the  $3T$  form is identical to that of  $2M_1$  muscovite, and, in addition, by comparing the structural parameters of the two forms, to seek reasons for the obvious preference by muscovite for the  $2M_1$  stacking sequence.

#### Specimen description

We obtained specimens of  $3T$  muscovite from Dr. M. ROSS, U.S. Geological Survey. This material is part of a sample collected by Dr. A. C. WATERS, who described it (in AXELROD and GRIMALDI, 1949) as “a white, nearly uniaxial muscovite (occurring) as veinlets and replacements in the granodiorite near the Sunrise Copper Prospect, Sultan Basin, Snohomish County, Washington”. WATERS stated that “The mica occurs as both fissure and ‘replacement veins’  $\frac{1}{4}$  to 1 inch thick which commonly appear along closely spaced partings or sheeting in the granodiorite.” He suggested that the mica may have formed by “selective replacement” of the granodiorite, and that “hot gases, following the sheeting in the granite rock, probably were the agents that formed the mica.”

AXELROD and GRIMALDI (1949) reported the following optical properties:

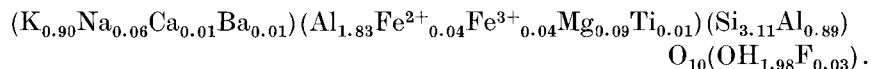
$$\begin{aligned} \text{Biaxial negative:} \quad \alpha &= 1.555 \pm 0.003 & 2V &= 15^\circ \pm 3^\circ \\ \beta &= 1.589 \pm 0.003 & Z &= a \\ \gamma &= 1.590 \pm 0.003 \end{aligned}$$

$$\begin{aligned} \text{Pleochroism feeble:} \quad X &= \text{pale yellow with some green} \\ Y = Z &= \text{deeper yellow with more green.} \end{aligned}$$

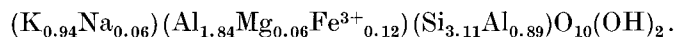
Under the polarizing microscope we observed that the mica appears as twinned  $4 \times 3 \times \frac{1}{2}$  mm aggregates with heavily striated and ruled surfaces. Small segments of uniform crystals form by cleaving along the rulings. Such grains with low birefringence show a  $2V$  of

2 to 5°, depending on the extent to which the crystals are bent. Our check on refractive indices gave the value  $\beta \leq \gamma = 1.592 \pm 0.002$  for Na light.

Calculating from a chemical analysis on the basis of 22 anionic charges, AXELROD and GRIMALDI (1949) gave the formula as:



This composition has a striking similarity to that of  $2M_1$  muscovite which was analyzed by RADOSLOVICH (1960). The formula of the latter is repeated here for comparison:



Although AXELROD and GRIMALDI (1949) recognized the appearance of trigonal symmetry on Laue and Weissenberg photographs, they suggested on the basis of asymmetry of diffuse streaks and the non-zero optic-axial angle that the true symmetry was monoclinic, space group  $C2$ . In reexamining the material, SMITH and YODER (1956) ascribed the diffuse streaks on Weissenberg photographs to stacking disorder and saw no evidence in the sharp x-ray reflections for lack of trigonal symmetry. They concluded that the mica is  $3T$ , with space group  $P3_112$  (or  $P3_212$ ).

### Space group and unit cell

Because of the ribbed, ruled nature of the flakes, which are often bent and warped, it is difficult to find single crystals of  $3T$  muscovite suitable for x-ray diffraction analysis. About 50 crystals that appeared optically uniform and free of mechanical distortion were examined by oscillation and rotation photographs. Zero-level Weissenberg photographs were taken of those that seemed promising, and the one that showed the least diffuse scattering and spot broadening was selected for intensity measurements. The  $a$ -(5.2 Å)-axis zero-level Weissenberg photograph of this crystal (Fig. 1) exhibits some diffuse scattering, indicating the presence of stacking disorder as well as mechanical distortion. Unfortunately, no better crystals could be found.

The space group was determined from a set of precession photographs taken along the  $c$ ,  $a$  (5.2 Å), and  $[12\cdot0]$  directions. The  $c$ -axis zero-level precession photograph displays plane point group  $6mm$ , whereas the first and second levels along the same direction show

plane point group  $3m$ . The  $a$ -axis zero-level precession photograph shows plane point group  $2mm$ , indicating that the possible 2-fold axis is normal to  $a$ . The  $[12\cdot0]$  zero-level precession photograph shows plane point group 2. The  $00\cdot l$  reflections with  $l \neq 3n$  are systematically absent, indicating the presence of a 3-fold screw axis. The diffraction symbol is thus  $\bar{3}mP3_1-$ ; since the 2-fold axis is normal to  $a$ , the space group is  $P3_112$  or its enantiomorph  $P3_212$ .

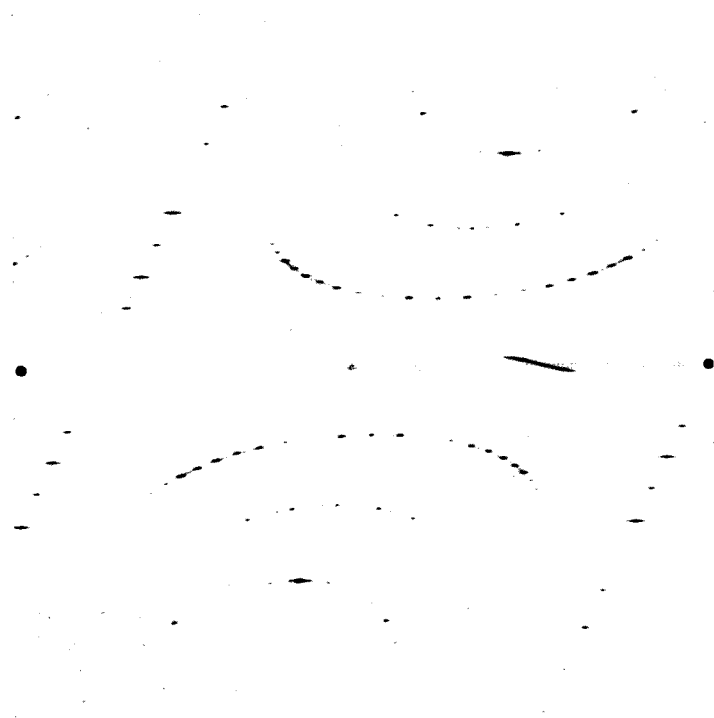


Fig.1. Weissenberg zero-level  $a$ -(5.2 Å)-axis photograph of  $3T$  muscovite showing diffuse scattering along the  $0kl$  reciprocal lattice rows

Precise unit-cell dimensions were obtained by least-squares refinement of data obtained with a precision back-reflection Weissenberg camera (BUERGER, 1942) using  $\text{CuK}\alpha$  radiation. The refinement was carried out using an IBM 7094 program (BURNHAM, 1962), which corrected for systematic errors due to film shrinkage, specimen absorption, and camera eccentricity. The following results were obtained:  $a = 5.1963 \pm 0.0004$  Å,  $c = 29.9705 \pm 0.0016$  Å, volume =  $70.084 \pm 0.13$  Å<sup>3</sup>.

### The 3*T* muscovite model

#### Polytype coordinates

Atomic coordinates of a 3*T* polytype model were derived from those of 2*M*<sub>1</sub> muscovite by considering the geometric relationships between the basic mica unit (the 1*M* form) and both the 2-layer and 3-layer forms (Fig. 2*a* and *b*). The orthohexagonal cell of 3*T* is described in terms of the monoclinic 2*M*<sub>1</sub> cell as follows:

$$\mathbf{a}_o = \mathbf{a}_2, \quad \mathbf{b}_o = \mathbf{b}_2, \quad \mathbf{c}_o = \frac{3}{2} \mathbf{c}_2 + \frac{1}{2} \mathbf{a}_2.$$

The hexagonal primitive cell of 3*T* is related to the orthohexagonal cell by

$$\mathbf{a}_P = \mathbf{a}_o, \quad \mathbf{b}_P = \frac{1}{2} \mathbf{b}_o - \frac{1}{2} \mathbf{a}_o, \quad \mathbf{c}_P = \mathbf{c}_o.$$

By combining these relations, the matrix for transforming atomic coordinates of a single mica layer from 2*M*<sub>1</sub> geometry to that of 3*T* becomes  $[11\frac{1}{3}/020/00\frac{2}{3}]$ . Using the atomic coordinates of 2*M*<sub>1</sub> determined by BURNHAM and RADOSLOVICH (1964), we thus obtained the

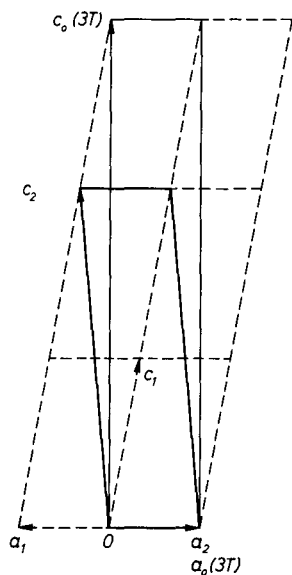
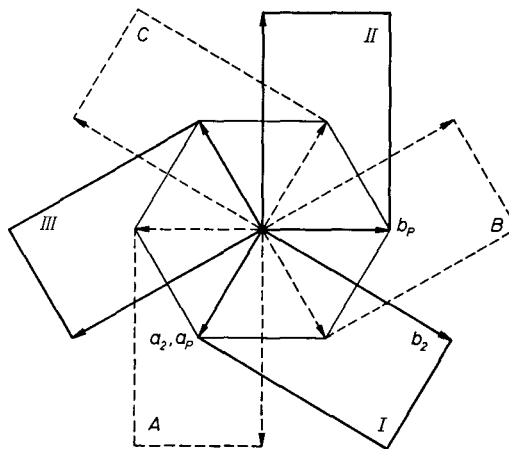
Fig. 2*a*Fig. 2*b*

Fig. 2*a*. Relationships between 1*M*, 2*M*<sub>1</sub>, and 3*T* muscovite unit cells as projected along the [010] direction

Fig. 2*b*. Relationships between 1*M* (dashed lines), 2*M*<sub>1</sub> (solid lines), and 3*T* muscovite unit cells as projected along the [001] direction

coordinates of atoms in an identical single mica layer referred to the  $3T$  unit cell. By itself this layer has  $C\bar{1}$  symmetry as it does in the  $2M_1$  structure; in the  $3T$  model the additional layers are generated by the operations of the  $3_1$  axis to yield a 3-layer polytype with space group  $P3_1$ .

The resulting atomic coordinates were used to calculate expected intensities of several  $0kl$  reflections. Comparison of these with the  $a$ -axis (5.2 Å) precession photograph showed qualitative agreement, indicating that a  $3T$  model in which the single mica layer is identical to that of  $2M_1$  muscovite is an acceptable starting point.

### Twinning

Polysynthetic twinning of  $1M$  muscovite following the common mica twin law— $180^\circ$  rotation around the  $[310]$  axis with composition plane  $(001)$ —may result in x-ray diffraction patterns similar to those of  $3T$  muscovite. SADANAGA and TAKÉUCHI (1961) pointed out that the twin and stacking operations become identical if the mica single layer possesses  $C2/m$  symmetry, and has a unit cell with  $b = a\sqrt{3}$ . Accordingly, the nature of a mica structure is clearly dependent on the frequency of the occurrence of the twin (= stacking) operation. If such an operation occurs regularly at unit-cell frequencies, a multi-layer polytype will result; if it occurs frequently but without regularity, the resulting structure would be described in terms of disorder due to numerous stacking faults; if it occurs only infrequently, the result would be termed a twin.

In the case of  $3T$  muscovite, the single mica layer possesses a 2-fold axis as explained previously. In the structure of  $2M_1$  muscovite, however, the 2-fold symmetry of the single mica layer is only approximate. For the sake of simplicity we will assume in the following discussion that 2-fold symmetry exists rigorously and that the stacking ( $120^\circ$  rotation about  $c^*$ ) and twin ( $180^\circ$  rotation about  $[310]$ ) operations are equivalent.

In the  $3T$  polytype, the atomic coordinates for successive mica layers are given by the operations from space group  $P3_1$ :

$$xyz; \bar{y}, x-y, \frac{1}{3} + z; y-x, \bar{x}, \frac{2}{3} + z.$$

The structure factor of the  $3T$  polytype can be expressed as

$$F_{3T} = \sum f_n e^{i2\pi(hx + ky + lz)} + \sum f_n e^{i2\pi(h'x + k'y + lz)} e^{i2\pi l/3} + \sum f_n e^{i2\pi(h''x + k''y + lz)} e^{i2\pi 2l/3} \quad (1)$$



where the summations are over the  $n$  atoms in the single mica layer, and the  $hk$  index transformation is given by the transpose of the matrix that transforms atomic coordinates. Thus the structure factor can be split into three terms related to each successive layer:

$$(F_{3T})_{hkl} = (F_1)_{hkl} + (F_2)_{h'k'l} \cdot e^{i2\pi l/3} + (F_3)_{h''k''l} \cdot e^{i2\pi 2l/3}. \quad (2)$$

If now the single mica layers are replaced by 1*M* crystals, the twin reciprocal lattice will be identical to that of the 3*T* polytype. The intensity distribution from the twin can be derived from Equation (2) by omitting phase shifts, since the individual crystals do not scatter coherently with respect to each other; hence

$$I_{\text{twin}} = \alpha (F_{hkl}^2)_{A(1M)} + \beta (F_{hkl}^2)_{B(1M)} + \gamma (F_{hkl}^2)_{C(1M)}, \quad (3)$$

where  $\alpha$ ,  $\beta$ , and  $\gamma$  are physical and geometrical factors. Note that the contributions of the first, second and third layers of the 3*T* polytype are now replaced by contributions from the *A*, *B*, and *C* monoclinic cells of 1*M* crystals making up the twin. The cell of 1*M* crystal is related to the hexagonal primitive cell of a corresponding mica layer of the 3*T* polytype (i.e. 1*M* crystal *A* to layer 1, 1*M* crystal *B* to layer 2, 1*M* crystal *C* to layer 3) by the matrix  $[R] = [0\bar{1}0/210/0\frac{1}{3}\frac{1}{3}]$ , as derived from relations shown in Fig. 2*b*. Note that layer 1 of the polytype is related to 1*M* cell *A* and not *B* or *C* because of the orientation requirements of the 2-fold axis parallel to *b* of the 1*M* cells.

The indices of the individual contributors to a twin reflection are related to the transformed indices of the corresponding polytype layer (see Equation 2) by the matrix  $[R]$  as follows:

$$\begin{aligned} \begin{vmatrix} h \\ k \\ l \end{vmatrix}_{A(1M)} &= [R] \begin{vmatrix} h \\ k \\ l \end{vmatrix}_{3T} \\ \begin{vmatrix} h \\ k \\ l \end{vmatrix}_{B(1M)} &= [R] \begin{vmatrix} h' \\ k' \\ l \end{vmatrix}_{3T} \\ \begin{vmatrix} h \\ k \\ l \end{vmatrix}_{C(1M)} &= [R] \begin{vmatrix} h'' \\ k'' \\ l \end{vmatrix}_{3T}. \end{aligned} \quad (4)$$

Using  $[R]$  as given above, we see that:

$$\begin{aligned} l_{A(1M)} &= \frac{(k+l)_{3T}}{3} \\ l_{B(1M)} &= \frac{(k'+l)_{3T}}{3} \\ l_{C(1M)} &= \frac{(k''+l)_{3T}}{3}. \end{aligned} \quad (5)$$

Thus for  $I_{\text{twin}}$  to be non-zero for any particular  $hkl$  of the twin reciprocal lattice, at least one of the relations given by Equation (5) must yield an integral value for  $l_{1M}$ . If, however, none of these relations gives integral values for  $l_{1M}$ , the intensity of that  $hkl$  reflection will be identically zero. It can be shown that if the conditions  $(h-k)_{3T} = 0 \pmod{3}$  and  $(k+l)_{3T} \neq 0 \pmod{3}$  are satisfied simultaneously, the relations given by (5) will all yield fractional values for  $l_{1M}$ . Reflections for which these conditions are satisfied lie along the  $S$  rows described by SADANAGA and TAKÉUCHI (1961) and will be missing if the crystal

Table 1  
*Intensities of twinned 1M muscovite and of the 3T polytype of muscovite*

Twin individuals		Observed	3T polytype					
$h$	$k$	$l$	$F_c^2$	$F_o^2$	$h$	$k$	$l$	
(0 2 0) <sub>A</sub>			176	77	104	1	0	0
(1 $\bar{1}$ 0) <sub>B</sub>			66	230	204	1	0	1
( $\bar{1}$ $\bar{1}$ 1) <sub>C</sub>			25	20	45	1	0	2
(0 2 1) <sub>A</sub>			23	63	47	1	0	3
(1 $\bar{1}$ 1) <sub>B</sub>			138	221	220	1	0	4
( $\bar{1}$ $\bar{1}$ 2) <sub>C</sub>			349	212	290	1	0	5
(0 2 2) <sub>A</sub>			503	410	689	1	0	6
(1 $\bar{1}$ 2) <sub>B</sub>			446	406	360	1	0	7
( $\bar{1}$ $\bar{1}$ 3) <sub>C</sub>			509	721	563	1	0	8
(0 2 3) <sub>A</sub>			193	144	217	1	0	9
(1 $\bar{1}$ 3) <sub>B</sub>			261	120	127	1	0	10
( $\bar{1}$ $\bar{1}$ 4) <sub>C</sub>			19	19	23	1	0	11
(0 2 4) <sub>A</sub>			92	5	6	1	0	12
(1 $\bar{1}$ 4) <sub>B</sub>			70	7	7	1	0	13
( $\bar{1}$ $\bar{1}$ 5) <sub>C</sub>			12	17	9	1	0	14
(0 2 5) <sub>A</sub>			27	21	33	1	0	15
(1 $\bar{1}$ 5) <sub>B</sub>			14	27	23	1	0	16
( $\bar{1}$ $\bar{1}$ 6) <sub>C</sub>			13	21	15	1	0	17
(0 2 6) <sub>A</sub>			94	48	66	1	0	18
(1 $\bar{1}$ 6) <sub>B</sub>			46	106	87	1	0	19
( $\bar{1}$ $\bar{1}$ 7) <sub>C</sub>			262	162	135	1	0	20
(0 2 7) <sub>A</sub>			48	43	85	1	0	21

is twinned. Since such reflections are observed (see Table 3), our crystal is not a twin.

We also tested the hypothesis of a polytype with "twinned domains" by examining the intensities of reflections along the  $(10l)_{3T}$  row. This is a  $T$  row in the terminology of SADANAGA and TAKÉUCHI (1961), and the reflections, while all observable, will nevertheless have different intensities depending on whether the crystal is a twin or a polytype. Intensity functions from Equations 2 and 3 were calculated on the IBM 7094 using a program developed by one of us (NG) with the  $3T$  polytype coordinates generated in the previous section. To afford suitable comparisons, intensities for the twin individuals were multiplied by 3. The results are given in Table 1. The  $F_{\text{obs}}$  values are those obtained from our crystal. Striking differences occur in intensity distribution along this row, with observed values in better agreement with those calculated for the  $3T$  polytype. In most cases the observed values do not lie between the two calculated values; hence it is unlikely that the crystal contains "twinned domains."

#### Intensity measurement and structure refinement

Intensities were measured by counter methods using our Supper-Pace automated single-crystal diffractometer. To minimize overlap of reflections due to: (1) the 30 Å  $c$  axis, (2) diffuseness caused by stacking faults, and (3) large mosaic spread, in part reflecting mechanical distortion of the crystal, we used V-filtered  $\text{CrK}\alpha$  x-radiation to record 463 accessible reflections with indices  $\pm h$ ,  $+k$ ,  $+l$ . We found that our Th-activated NaI scintillation detector, linear amplifier, and PHA circuitry (set to accept 90% of the incoming radiation) operate satisfactorily with this wavelength. Our intensity collection and data-processing procedures have already been described (GÜVEN and BURNHAM, 1966) and need not be repeated here. Intensity data were converted to observed structure factors by applying the standard Lorentz and polarization corrections, and a precise absorption correction was calculated on the IBM 7094 using numerical integration techniques (BURNHAM, 1966). Several reflections, whose intensities were inaccurately determined because of superposition or diffuse streaking problems, had to be disregarded. Thus only 341 reflections, listed in Table 3, could be used for the refinement.

Full-matrix least-squares refinement of the  $3T$  structure was carried out on the IBM 7094 computer using a program written by

PREWITT (1962) and modified by one of us (CB) to accept analytic expressions for atomic scattering curves. All atoms were considered to be fully ionized, and the scattering curve for  $O^{-2}$  was used for  $OH^{-}$ . Both real and imaginary anomalous dispersion corrections were applied throughout the refinement. The technical aspects of our use of scattering factors and anomalous dispersion corrections are analogous to those described by PREWITT and BURNHAM (1966).

To eliminate constraints on atomic positions in the single mica layer we initiated the refinement in space group  $P3_1$ , with 19 atoms in the asymmetric unit. If the assumption of polytypism between  $2M_1$  and  $3T$  muscovites is strictly valid, the space group of the  $3T$  form must be  $P3_1$ , since the single layers of  $2M_1$  muscovite possess symmetry  $C\bar{1}$  (BURNHAM and RADOSLOVICH, 1964; GÜVEN, 1967).

After three cycles of refinement, the discrepancy factors for the  $P3_1$  model were reduced to 0.094 (unweighted  $R$ ) and 0.062 (weighted  $R$ ). Subsequent refinement of isotropic thermal parameters gave a negative temperature factor for  $OH^{-}$ . At this stage strong correlation coefficients existed between parameters of some pairs of atoms which can be related by a 2 or  $\bar{1}$  operation in the single layer. The coordinates of an apparent inversion center in the single layer of  $3T$  muscovite were calculated, and tests for the presence of this center showed that the pairs of atoms  $Si_1$ ,  $Si_2$ ,  $O_c$ ,  $O_e$ , and  $O_d$  were clearly off their centrosymmetric sites. Thus the single layer of  $3T$  muscovite does not possess an inversion center in contrast with that of  $2M_1$ . Similarly we tested for the presence of the 2-fold axis, which must be present if the space group is indeed  $P3_12$ . With the exception of two basal oxygen atoms the agreement was satisfactory, and subsequent refinement was carried out in space group  $P3_12$ . Discrepancy factors resulting from refinement in both space groups are summarized in Table 2; comparison shows that group  $P3_12$  is fully justified.

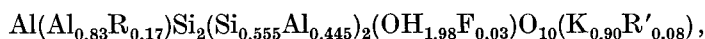
Refinement of isotropic temperature factors was successfully run through three cycles in this space group, and a preliminary computation of the bond lengths showed the following mean values:

$$\begin{aligned}T_1-O &= 1.666 \pm 0.017 \text{ \AA} \\T_2-O &= 1.615 \pm 0.017 \text{ \AA} \\Al_1-O &= 1.967 \pm 0.013 \text{ \AA} \\Al_2-O &= 1.910 \pm 0.012 \text{ \AA}.\end{aligned}$$

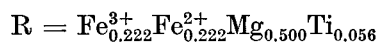
Table 2. *Discrepancy factors for the two possible space groups of 3T muscovite based on 341 reflections*

	<i>P</i> 3 <sub>1</sub>	<i>P</i> 3 <sub>1</sub> 12
Unweighted $R \left( = \frac{\sum  F_o - F_c }{\sum F_o} \right)$ for all observations	10.4	9.9
Weighted $R \left( = \left[ \frac{\sum w (\Delta F)^2}{\sum w F_o^2} \right]^{\frac{1}{2}} \right)$ for all observations	6.6	6.3
Unweighted $R$ for 318 unrejected reflections	9.4	9.1
Weighted $R$ for 318 unrejected reflections	6.2	6.1
Standard error of fit $[\sum w (F_o - F_c)^2 / (m - n)]^{1/2}$	13.016	12.448

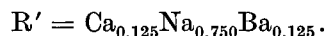
Comparison of the tetrahedral bond lengths with those given by SMITH and BAILEY (1963) indicates that the  $T_2$  tetrahedron contains only Si, whereas the  $T_1$  tetrahedron contains about 35% Al. The octahedral distances, compared with the corresponding values given by BURNHAM and RADOSLOVICH (1964) and by GÜVEN (1967) for 2*M*<sub>1</sub> muscovite, indicate that the Al<sub>2</sub> octahedron has no noticeable isomorphic replacement, whereas the Al<sub>1</sub> octahedron contains larger cations and is possibly distorted. We modified the chemical formula given by AXELROD and GRIMALDI (1949), assigning appropriate site occupancies according to the following scheme:



where



and



Final refinement was carried out with the 341 reflections listed in Table 3 using a subroutine which rejected reflections with  $|F_o - F_c| > 6.0$ . The refinement converged after six cycles to an unweighted  $R$  of 0.064 and weighted  $R$  of 0.024 for 280 reflections that were not rejected. The calculated  $F$ 's at  $R = 0.064$  are given in Table 3 (corrected for anomalous dispersion). Of these  $F$ 's, 129 are redundant since they are related by the 2-fold axis and subsequent inversion. Since we corrected them for anomalous dispersion, these reflections are instead treated as independent\*. Further, 57  $F$ 's which

\* A test of absolute orientation using inverted atomic coordinates in space group *P*3<sub>2</sub>12 yielded  $R$  values of .069 (unweighted) and .026 (weighted), as compared with .064 and .024 using the coordinates of Table 4 in space group *P*3<sub>1</sub>12.

Table 3. Observed and calculated structure factors of 3T muscovite ( $F_o$ 's are corrected for anomalous dispersion)

h	k	l	$F_o$	$F_c$	h	k	l	$F_o$	$F_c$	h	k	l	$F_o$	$F_c$	h	k	l	$F_o$	$F_c$
0	0	6	60.8	57.7	-3	0	0	188.0	196.3	-1	1	23	11.0	12.4	-1	2	19	178.5	178.0
0	0	9	142.2	129.2	3	0	3	44.7	45.2	-1	1	24	11.2	13.8	-1	2	20	25.5	25.0
0	0	12	65.9	65.6	-3	0	5	42.1	44.7	2	1	1	26.5	30.6	-1	2	21	2.9	2.3
0	0	15	187.4	176.7	3	0	7	5.8*	9.5	-2	1	2	152.1	148.9	-1	2	22	42.4	43.1
0	0	18	24.7	17.0	-3	0	5	5.8*	9.5	-2	1	5	95.6	95.0	-2	2	0	39.1	41.7
0	0	21	67.8	67.1	3	0	6	5.4	9.3	-2	1	6	14.3	12.2	2	2	1	75.7	85.2
0	0	24	104.4	103.0	-3	0	6	8.0*	9.7	-2	1	7	10.5	9.8	-2	2	1	25.6	36.4
1	0	0	27.5	28.2	3	0	7	5.7	8.7	-2	1	8	27.9	30.8	-2	2	3	46.4	49.3
-1	0	0	27.8	30.4	-3	0	7	9.2	9.5	-2	1	8	109.4	127.3	2	2	4	6.8*	6.3
1	0	1	47.8	51.4	3	0	8	10.2	15.7	2	1	9	26.9	30.7	-2	2	6	49.4	45.1
-1	0	1	49.0	49.2	-3	0	8	12.2	15.8	-2	1	9	11.5	18.2	-2	2	7	22.4	11.9
1	0	2	14.0	18.2	3	0	9	35.2	33.1	2	1	10	34.4	39.5	2	2	8	21.5	23.2
-1	0	2	19.9	22.1	-3	0	9	33.4	33.0	-2	1	10	5.8*	1.5	-2	2	8	17.5	28.8
1	0	3	25.0	33.4	3	0	10	7.3*	2.0	2	1	11	18.8	30.6	2	2	9	2.2	9.0
1	0	4	46.8	50.3	-3	0	10	6.4*	3.2	2	1	12	15.7	14.3	-2	2	9	22.4	23.9
-1	0	4	52.9	52.3	3	0	11	20.2	24.5	-2	1	12	7.4*	3.0	-2	2	12	18.5	28.4
1	0	6	65.6	71.5	-3	0	11	24.2	24.8	2	1	14	17.4	20.5	-2	2	14	30.7	30.5
-1	0	6	70.4	72.7	-3	0	12	87.4	93.1	-2	1	14	124.0	152.5	-2	2	15	17.0	15.7
1	0	7	63.4	73.5	-3	0	12	89.8	93.0	2	1	15	12.0	11.1	-2	2	16	48.7	45.8
1	0	8	84.5	83.7	3	0	13	35.1	34.5	-2	1	15	18.0	19.5	-2	2	17	32.6	32.5
-1	0	8	94.1	84.0	-3	0	13	37.8	36.0	2	1	16	21.7	24.1	-2	2	18	84.2	83.5
-1	0	9	42.2	39.6	3	0	14	28.8	28.5	-2	1	16	5.1*	5.0	-2	2	19	36.3	36.0
1	0	10	34.5	31.5	-3	0	14	27.7	27.4	2	1	17	2.9	9.9	-2	2	20	44.2	4.6
-1	0	10	33.5	32.9	3	0	15	56.9	55.3	2	1	18	11.0	13.7	-2	2	21	45.5	45.9
1	0	11	13.6	10.2	-3	0	15	56.7	55.2	-2	1	18	7.3	11.4	-3	2	1	30.3	30.6
-1	0	11	8.2*	10.3	0	1	0	27.2	30.4	-2	1	19	6.5	8.4	-3	2	6	64.9	60.6
1	0	12	7.2*	4.9	0	1	1	47.6	49.2	-2	1	21	7.0	6.4	-3	2	7	44.7	44.7
-1	0	12	7.5*	6.2	-3	0	12	24.2	28.1	-2	1	22	11.5	3.0	-3	2	8	33.4	59.6
1	0	13	11.9	11.2	0	1	3	26.7	29.5	-3	1	1	27.3	29.5	-3	2	9	31.4	30.7
-1	0	13	12.9	9.6	0	1	4	53.6	51.9	-3	1	4	22.6	28.6	-3	2	10	37.4	39.5
1	0	14	13.0	13.0	0	1	5	53.6	52.3	3	1	5	72.9	74.1	-3	2	11	24.0	30.6
-1	0	14	13.4	15.2	0	1	6	67.8	72.7	-3	1	5	36.4	36.2	-3	2	12	14.6	14.3
1	0	15	17.0	17.7	0	1	7	65.3	71.9	3	1	6	33.3	27.3	-3	2	13	8.7	9.0
-1	0	15	17.8	14.8	0	1	8	69.3	84.0	3	1	7	33.7	44.2	-3	2	14	17.7	20.5
1	0	16	16.3	13.4	0	1	9	35.5	39.6	-3	1	7	29.7	40.4	-3	2	15	11.7	11.1
-1	0	16	16.3	15.9	0	1	10	30.0	32.9	-3	1	8	24.2	33.2	-3	2	16	22.3	24.1
1	0	17	14.3	20.1	0	1	11	9.6	10.3	-3	1	9	20.4	28.5	-3	2	17	10.2	9.9
-1	0	17	9.8	15.0	0	1	12	5.3*	6.2	-3	1	13	6.5*	8.4	0	3	0	181.7	196.3
1	0	18	21.9	20.5	0	1	13	9.7	9.6	-3	1	14	11.0	21.6	0	3	3	42.9	44.7
-1	0	18	24.8	22.5	0	1	14	12.6	15.2	-3	1	15	7.5	9.3	0	3	5	5.4*	9.5
1	0	19	32.3	35.7	0	1	15	11.2	14.8	-3	1	17	8.5	10.5	0	3	6	5.3*	9.7
-1	0	19	35.3	34.3	0	1	16	11.9	15.9	-3	1	18	8.5	15.3	0	3	8	14.7	15.8
1	0	20	40.1	42.1	0	1	17	7.7	15.0	0	2	0	43.0	37.0	0	3	9	33.1	33.3
-1	0	20	39.8	42.4	0	1	18	19.3	22.5	0	2	1	25.0	34.4	0	3	10	7.2*	3.2
1	0	21	20.7	23.0	0	1	19	27.4	34.3	0	2	2	22.7	19.7	0	3	11	25.8	24.8
-1	0	21	22.1	22.4	0	1	21	17.8	22.4	0	2	3	48.4	48.4	0	3	12	93.1	93.0
1	0	22	33.9	32.0	0	1	22	27.1	32.0	0	2	4	44.8	45.5	-2	3	13	34.8	36.0
-1	0	22	33.1	32.0	0	1	23	10.6	10.5	0	2	8	15.8	23.4	0	3	14	27.5	27.4
1	0	23	11.5	12.4	0	1	24	12.3	15.5	0	2	9	21.6	29.1	0	3	15	55.1	55.2
-1	0	23	13.2	10.5	-1	1	1	48.7	51.4	0	2	10	20.8	19.4	-1	3	1	13.3	13.0
1	0	24	15.9	13.8	1	1	2	130.6	148.9	0	2	13	33.5	35.2	1	3	6	36.1	28.5
-1	0	24	18.0	15.5	-1	1	2	18.1	18.2	-1	2	11	29.6	29.6	-1	3	6	33.4	59.6
2	0	0	40.9	41.7	-1	1	3	30.9	33.4	0	2	15	21.8	18.1	-1	3	7	43.5	34.1
-2	0	0	39.9	42.3	-1	1	4	50.4	50.3	0	2	16	44.1	44.5	-1	3	8	51.8	62.0
2	0	1	26.0	36.4	1	1	5	103.9	95.0	0	2	17	32.4	34.2	-1	3	10	10.9	1.4
-2	0	1	24.3	34.4	-1	1	5	50.1	53.9	0	2	18	83.2	83.0	-1	3	11	8.7	12.2
2	0	2	15.8	18.5	-1	1	6	62.0	71.5	0	2	19	37.4	37.4	-1	3	12	22.5	24.0
-2	0	2	15.5	19.7	1	1	7	9.7	9.8	0	2	20	42.6	42.1	-1	3	13	21.2	21.1
2	0	3	50.6	49.3	-1	1	7	62.2	73.5	0	2	21	47.9	46.6	-1	3	14	17.1	19.3
-2	0	3	47.3	48.4	1	1	8	124.9	127.3	1	2	1	28.5	29.5	-1	3	15	17.0	16.5
2	0	6	41.8	45.1	1	1	9	11.9	18.2	1	2	3	20.8	29.3	-1	3	16	14.8	16.0
-2	0	6	43.7	45.5	-1	1	9	36.7	39.6	1	2	4	28.9	28.6	-1	3	17	2.8	3.9
2	0	8	23.2	23.4	1	1	10	6.2*	1.5	-1	2	4	96.0	93.4	-2	3	3	31.3	22.3
-2	0	8	24.8	23.9	-1	1	10	32.1	31.5	-1	2	6	6.7	7.6	-2	3	6	44.7	60.1
2	0	10	19.9	19.4	1	1	11	36.6	38.5	-1	2	7	45.7	44.7	-2	3	7	33.7	32.3
-2	0	11	30.6	36.0	-1	1	11	11.4	10.2	1	2	8	25.3	33.2	-2	3	10	9.2	2.9
2	0	11	34.4	38.6	1	1	12	8.6*	3.0	-1	2	8	9.5	7.3	-2	3	11	39.1	33.3
-2	0	12	16.4	28.4	-1	1	12	5.4*	4.9	1	2	9	26.9	28.5	-2	3	12	21.3	23.1
2	0	12	18.1	25.4	1	1	13	17.6	22.7	-1	2	9	18.4	17.8	-2	3	13	21.1	23.6
-2	0	14	30.7	30.5	-1	1	13	8.3	11.2	1	2	10	37.2	39.9	-2	3	14	15.3	17.6
2	0	15	17.5	15.7	1	1	14	140.2	152.5	-1	2	10	109.0	109.5	-2	3	15	16.2	18.5
-2	0	15	18.5	18.1	1	1	15	21.7	19.5	1	2	11	13.3	29.3	-2	3	16	13.8	13.5
2	0	16	44.4	45.8	-1	1	15	13.6	17.7	-1	2	11	25.8	24.7	-2	3	17	6.2	8.1
-2	0	16	47.2	44.5	1	1	16	4.8	5.0	1	2	12	16.6	15.6	-3	3	0	182.3	196.6
2	0	17	34.7	32.5	-1	1	16	9.7	13.4	-1	2	12	21.5	17.8	-3	3	5	8.5	9.5
-2	0	17	35.8	34.2	1	1	17	65.2	74.3	1	2	13	7.9	8.4	-3	3	6	10.3	9.3
2	0	18	85.5	83.5	-1	1	17	8.5	20.1	-1	2	13	95.7	93.8	-3	3	7	11.1	9.7
-2	0	18	85.1	83.0	1	1	18	6.9	11.4	1	2	14	20.0	21.6	-3	3	8	14.8	15.7
2	0	19	39.0	36.0	-1	1	18	17.6	20.5	-1	2	14	18.0	16.2	-3	3	9	29.5	33.1
-2	0	19	38.5	37.4	1	1	19	4.5*	8.4	-1	2	15	19.3	19.1	-3	3	10	7.9*	2.0
2																			

Table 4. Atomic coordinates in 3T muscovite, space group  $P3_112$ , origin at  $3_112$

Position	Atom	$x$	$\sigma(x)$	$y$	$\sigma(y)$	$z$	$\sigma(z)$	$B$	$\sigma(B)$
3a	Al <sub>1</sub>	-0.230 ± 0.001		0.230 ± 0.001		1/3		0.95 ± 0.17	
3a	Al <sub>2</sub>	0.100 ± 0.001		-0.100 ± 0.001		1/3		0.74 ± 0.19	
3b	K	0.130 ± 0.001		-0.130 ± 0.001		5/6		1.73 ± 0.10	
6c	O <sub>a</sub>	0.750 ± 0.004		0.178 ± 0.003		-0.0357 ± 0.0004		1.53 ± 0.43	
6c	O <sub>b</sub>	0.522 ± 0.003		0.566 ± 0.004		-0.0363 ± 0.0004		0.40 ± 0.35	
6c	OH	0.112 ± 0.004		-0.085 ± 0.004		-0.0337 ± 0.0002		0.39 ± 0.19	
6c	T <sub>1</sub>	0.796 ± 0.002		0.200 ± 0.002		-0.0894 ± 0.0001		0.19 ± 0.20	
6c	T <sub>2</sub>	0.462 ± 0.002		0.550 ± 0.002		-0.0895 ± 0.0001		0.65 ± 0.20	
6c	O <sub>c</sub>	0.666 ± 0.004		0.857 ± 0.004		-0.1110 ± 0.0003		0.74 ± 0.22	
6c	O <sub>d</sub>	0.140 ± 0.005		0.451 ± 0.004		-0.1058 ± 0.0004		0.80 ± 0.30	
6c	O <sub>e</sub>	0.563 ± 0.004		0.311 ± 0.004		-0.1098 ± 0.0003		0.17 ± 0.27	

factors are possibly related to the stacking disorder described previously.

Final interatomic distances and angles were calculated using the IBM 7094 program ORFFE (BUSING *et al.*, 1964), and the results

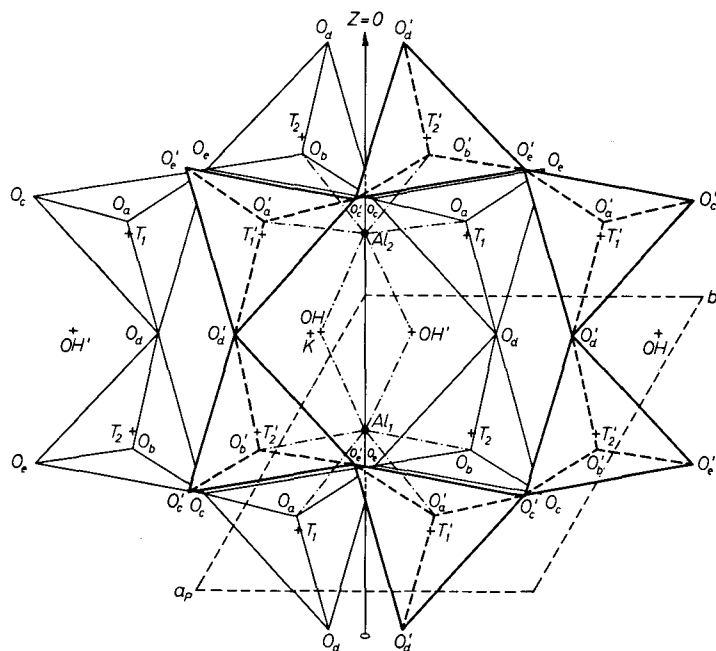


Fig. 3. Single mica layer of 3T muscovite projected on (001). Thick solid and dashed lines: upper tetrahedral layers. Thin solid lines: lower tetrahedral layers. Dash-dot lines: octahedral polyhedra

Table 5. *Interatomic distances in 3T muscovite*  
(See Fig. 3 for atom designation)

$T_1$ tetrahedron:		$T_2$ tetrahedron:	
$T_1-O_a$	$1.622 \pm 0.014 \text{ \AA}$	$T_2-O_b$	$1.619 \pm 0.012 \text{ \AA}$
$T_1-O_c$	$1.690 \pm 0.018$	$T_2-O_c$	$1.545 \pm 0.017$
$T_1-O_d$	$1.675 \pm 0.022$	$T_2-O_a$	$1.563 \pm 0.021$
$T_1-O_e$	$1.698 \pm 0.015$	$T_2-O_e$	$1.686 \pm 0.016$
Mean $T_1-O$	$1.671 \pm 0.009$	Mean $T_2-O$	$1.603 \pm 0.008$
$O_a-O_c$	$2.709 \pm 0.019 \text{ \AA}$	$O_b-O_c$	$2.593 \pm 0.016 \text{ \AA}$
$O_a-O_d$	$2.768 \pm 0.022$	$O_b-O_a$	$2.731 \pm 0.020$
$O_a-O_e$	$2.653 \pm 0.016$	$O_b-O_e$	$2.634 \pm 0.016$
$O_c-O_d$	$2.831 \pm 0.024$	$O_c-O_a$	$2.488 \pm 0.024$
$O_c-O_e$	$2.674 \pm 0.024$	$O_c-O_e$	$2.606 \pm 0.025$
$O_d-O_e$	$2.713 \pm 0.026$	$O_e-O_a$	$2.638 \pm 0.023$
Mean $O-O$	$2.725 \pm 0.009$	Mean $O-O$	$2.615 \pm 0.009$
$Al_1$ octahedron:		$Al_2$ octahedron:	
$Al_1-O_a$	$1.971 \pm 0.019 \text{ \AA}$	$Al_2-O_b'$	$1.943 \pm 0.015 \text{ \AA}$
$Al_1-O_b'$	$1.941 \pm 0.015$	$Al_2-O_a$	$1.918 \pm 0.016$
$Al_1-O_b$	$1.941 \pm 0.015$	$Al_2-O_b$	$1.943 \pm 0.015$
$Al_1-O_a'$	$1.971 \pm 0.019$	$Al_2-O_a'$	$1.918 \pm 0.015$
$Al_1-OH$	$2.002 \pm 0.017$	$Al_2-OH$	$1.878 \pm 0.015$
$Al_1-OH'$	$2.002 \pm 0.017$	$Al_2-OH'$	$1.878 \pm 0.015$
Mean $Al_1-O$	$1.971 \pm 0.007$	Mean $Al_2-O$	$1.913 \pm 0.006$
Unshared:		Unshared:	
$O_a-O_a'$	$2.961 \pm 0.031 \text{ \AA}$	$OH'-O_a$	$2.775 \pm 0.020 \text{ \AA}$
$O_b'-OH$	$2.918 \pm 0.018$	$O_a'-OH$	$2.775 \pm 0.020$
$OH'-O_b$	$2.918 \pm 0.018$	$O_b-O_b'$	$2.972 \pm 0.026$
Mean $O-O$	$2.932 \pm 0.013$	Mean	$2.841 \pm 0.013$
unshared		unshared	
Shared:		Shared:	
$OH-OH'$	$2.492 \pm 0.019 \text{ \AA}$	$OH-OH'$	$2.492 \pm 0.019 \text{ \AA}$
$O_a-O_b'$	$2.453 \pm 0.012$	$O_a-O_b'$	$2.453 \pm 0.012$
$O_b-O_a'$	$2.453 \pm 0.012$	$O_b-O_a'$	$2.453 \pm 0.012$
Mean	$2.466 \pm 0.008$	Mean	$2.466 \pm 0.008$
shared		shared	
Interlayer cation:		Interlayer cation:	
$K-O_c$	$2.900 \pm 0.014 \text{ \AA}$	$K-O_c$	$3.283 \pm 0.014 \text{ \AA}$
$K-O_e$	$2.839 \pm 0.015$	$K-O_e$	$3.385 \pm 0.015$
$K-O_d$	$2.864 \pm 0.015$	$K-O_d$	$3.502 \pm 0.014$
Mean $K-O$	$2.868 \pm 0.009$	Mean $K-O$	$3.390 \pm 0.008$
$K-OH$	$3.997 \pm 0.007 \text{ \AA}$	$K-OH$	$3.997 \pm 0.007 \text{ \AA}$



Table 6. *Interatomic angles in 3T muscovite*  
(Central atom is vertex)

<i>T</i> <sub>1</sub> tetrahedron:		<i>T</i> <sub>2</sub> tetrahedron:	
O <sub>c</sub> - <i>T</i> <sub>1</sub> -O <sub>d</sub>	114.59 ± 0.76°	O <sub>c</sub> - <i>T</i> <sub>2</sub> -O <sub>d</sub>	106.36 ± 0.78°
O <sub>e</sub> - <i>T</i> <sub>1</sub> -O <sub>c</sub>	104.23 ± 0.92	O <sub>c</sub> - <i>T</i> <sub>2</sub> -O <sub>e</sub>	107.50 ± 0.83
O <sub>e</sub> - <i>T</i> <sub>1</sub> -O <sub>d</sub>	107.12 ± 0.93	O <sub>a</sub> - <i>T</i> <sub>2</sub> -O <sub>e</sub>	108.58 ± 0.88
O <sub>a</sub> - <i>T</i> <sub>1</sub> -O <sub>e</sub>	106.06 ± 0.90	O <sub>b</sub> - <i>T</i> <sub>2</sub> -O <sub>c</sub>	110.06 ± 0.83
O <sub>a</sub> - <i>T</i> <sub>1</sub> -O <sub>c</sub>	109.75 ± 0.79	O <sub>b</sub> - <i>T</i> <sub>2</sub> -O <sub>d</sub>	118.23 ± 0.79
O <sub>a</sub> - <i>T</i> <sub>1</sub> -O <sub>d</sub>	114.21 ± 0.75	O <sub>b</sub> - <i>T</i> <sub>2</sub> -O <sub>e</sub>	105.69 ± 0.85
Mean O- <i>T</i> <sub>1</sub> -O	109.32 ± 0.35	Mean O- <i>T</i> <sub>2</sub> -O	109.40 ± 0.34
Angles between basal oxygens:		Amount of rotation from 120°	
O <sub>e</sub> -O <sub>c</sub> -O <sub>d</sub>	141.24 ± 0.52°		21.24°
O <sub>a</sub> -O <sub>e</sub> -O <sub>c</sub>	143.81 ± 0.60		23.81
O <sub>c</sub> -O <sub>d</sub> -O <sub>e</sub>	145.52 ± 0.58		25.52
O <sub>c</sub> -O <sub>d</sub> -O <sub>e</sub>	94.97 ± 0.38		25.03
O <sub>e</sub> -O <sub>c</sub> -O <sub>d</sub>	97.23 ± 0.41		22.77
O <sub>a</sub> -O <sub>e</sub> -O <sub>c</sub>	96.31 ± 0.38		23.69
		Mean	23.68 ± 0.20

are given in Tables 5 and 6. The configuration of the single mica layer is shown in projection on (001) in Fig. 3.

To check our refinement results the three-dimensional electron-density distribution and the difference electron density ( $\rho_o - \rho_c$ ) were computed using an IBM 7090 program (SLY *et al.*, 1962). The Fourier and difference-Fourier maps clearly show that there is no noticeable electron density in the vacant octahedral sites. Further, the difference-Fourier map confirms the refined structure.

### Comparison of 3*T* and 2*M*<sub>1</sub> muscovite structures

The differences between these two forms of muscovite consist essentially of (a) substitutional order-disorder of the tetrahedral and octahedral cations and (b) the distortions in the two structures.

#### a) Substitutional order-disorder

Interatomic distances in 3*T* muscovite and in the well-refined 2*M*<sub>1</sub> structures are summarized in Table 7. There is a noticeable "partial ordering" in both tetrahedra and octahedra of 3*T* muscovite, with Al restricted to the *T*<sub>1</sub> tetrahedron and Fe, Mg, and Ti to the Al<sub>1</sub> octahedron. In 2*M*<sub>1</sub> muscovites there is no such ordering.

Table 7. Comparison of the tetrahedral and octahedral mean interatomic distances in  $3T$  and  $2M_1$  muscovite

$3T$ muscovite		$2M_1$ muscovite	
		(BURNHAM and RADOSLOVICH, 1964)	(GÜVEN, 1967)
$T_1$ tetrahedron			
$T_1$ -O	1.671 Å	1.645 Å	1.643 Å
O-O	2.725	2.685	2.682
$T_2$ tetrahedron			
$T_2$ -O	1.603	1.645	1.643
O-O	2.615	2.685	2.682
$Al_1$ octahedron			
$Al_1$ -O	1.971	1.923	1.932
O-O (unshared)	2.932	2.824	2.891
$Al_2$ octahedron			
$Al_2$ -O	1.913	1.923	1.932
O-O (unshared)	2.841	2.824	2.891
shared			
OH-OH	2.492	2.370	2.402
O-O	2.453	2.446	2.454

## b) Distortions

Comparing the interatomic distances in  $3T$  muscovite and the wellrefined structures of  $2M_1$  muscovite (BURNHAM and RADOSLOVICH, 1964; GÜVEN, 1967) we found that individual tetrahedra are more regular in the  $2M_1$  than in the  $3T$  structure. However, the linkage of the tetrahedra results in slightly greater structural distortion in  $2M_1$  than in  $3T$ . These distortions may be divided into two types: those in the plane of the layers and those normal to the layers.

Tetrahedra rotate about axes normal to the layer, destroying the ideal hexagonal-sheet configuration and forming pseudoditrigonal rings of tetrahedra. The amount of rotation is obtained by comparing the observed interatomic angles between basal oxygen atoms (Table 6) to the  $120^\circ$  values found in ideal hexagonal rings. The tetrahedral rotations have a mean value of  $11.84 \pm 0.10^\circ$  in  $3T$  muscovite, since the rotations of two adjacent tetrahedra contribute to the total deviation from  $120^\circ$ . The corresponding rotations in  $2M_1$  muscovite have a mean value of  $11.37 \pm 0.04^\circ$  (GÜVEN, 1967).

The tetrahedral distortions normal to the plane of the mica sheet are shown by the difference of the *z* coordinates of the basal oxygens. In both structures, basal oxygen atoms O<sub>c</sub> and O<sub>e</sub> are coplanar whereas O<sub>d</sub> occupies a position off this plane towards the vacant octahedral site. The amount of "tetrahedral tilt" can be calculated according to:

$$\Delta z = \left[ \frac{z_{O_c} + z_{O_e}}{2} - z_{O_d} \right] \cdot c \cdot \sin \beta.$$

The tilt,  $\Delta z$ , is 0.23 Å in both the 2*M*<sub>1</sub> muscovite structure refined by GÜVEN (1967), and the Na-rich 2*M*<sub>1</sub> muscovite structure determined by BURNHAM and RADOSLOVICH (1964). In the 3*T* structure, however, the tilt is 0.14 ± 0.02 Å showing that basal oxygen layers are less corrugated than those in 2*M*<sub>1</sub> muscovite.

The tetrahedral cations are coplanar in both the 2*M*<sub>1</sub> and 3*T* structures. Also the extent of octahedral flattening is essentially the same in both structures. As seen in Table 7, the shared OH—OH edge in 2*M*<sub>1</sub> muscovites is noticeably contracted and is shorter than the other shared edges. Corresponding shared octahedral edges in 3*T* muscovite, show also similar differences.

### Conclusion

The concept of polytypism, as developed in studies of different forms of substances like SiC, CdI<sub>2</sub> and ZnS is based on different ways of stacking ideally close-packed equivalent layers (VERMA and KRISHNA, 1966). As shown above, the single layer of 3*T* muscovite is not equivalent to the single layer of 2*M*<sub>1</sub> muscovite; hence, these two structures cannot be considered polytypes. However, both single layers bear an interesting relation to an ideal undistorted mica single layer with a disordered cation distribution, whose symmetry is *C*2/*m*. In 2*M*<sub>1</sub> muscovite the mirror plane is destroyed by distortions, and the symmetry of the single layer is reduced to *C* $\bar{1}$ , while in 3*T* muscovite the inversion center is destroyed by substitutional ordering, and the symmetry of the single layer becomes *C*2. Thus, both single layers are derivatives (BUERGER, 1947) of the ideal mica layer. We propose therefore to term the two muscovite structures *polymorphs* with *derivative single layers*.

### Acknowledgments

Dr. M. Ross of the U.S. Geological Survey gave us the sample for the structure analysis, and we enjoyed several very constructive discussions with him. His review of the final manuscript has greatly improved it. It is a pleasure to thank Dr. H. S. YODER, JR., for many encouraging suggestions throughout this work and for his review of the final manuscript. Dr. G. DONNAY also critically reviewed the manuscript.

### References

- J. M. AXELROD and F. S. GRIMALDI (1949), Muscovite with small optic axial angle. *Amer. Mineralogist* **34**, 559–572.
- M. J. BUERGER (1942), X-ray crystallography. John Wiley and Sons, New York.
- M. J. BUERGER (1947), Derivative crystal structures. *J. chem. Physics* **15**, 1–16.
- C. W. BURNHAM (1962), Lattice constant refinement. *Carnegie Inst. Wash. Year Book* **61**, 132–135.
- C. W. BURNHAM (1966), Computation of absorption corrections, and the significance of end effect. *Amer. Mineralogist* **51**, 159–167.
- C. W. BURNHAM and E. W. RADOSLOVICH (1964), Crystal structures of coexisting muscovite and paragonite. *Carnegie Inst. Wash. Year Book* **63**, 232–236.
- W. R. BUSING, K. O. MARTIN and H. A. LEVY (1964), ORFFE, a Fortran crystallographic function and error program. Oak Ridge National Laboratory, ORNL-TM-306.
- L. GATINEAU (1963), Localisation des remplacements isomorphiques dans la muscovite. *Compt. Rend. Acad. Sci. Paris* **256**, 4648–4649.
- N. GÜVEN (1967), The crystal structures of  $2M_1$  phengite and  $2M_1$  muscovite. *Carnegie Inst. Wash. Year Book* **66** (in press).
- N. GÜVEN and C. W. BURNHAM (1966), The crystal structure of  $3T$  muscovite. *Carnegie Inst. Wash. Year Book* **65**, 290–293.
- S. B. HENDRICKS and M. E. JEFFERSON (1939), Polymorphism of micas with optical measurements. *Amer. Mineralogist* **24**, 729–771.
- W. W. JACKSON and J. WEST (1930), The crystal structure of muscovite,  $KAl_2(AlSi_3)O_{10}(OH)_2$ . *Z. Kristallogr.* **76**, 211–227.
- C. T. PREWITT (1962), Unpublished least-squares computer program.
- C. T. PREWITT and C. W. BURNHAM (1966), The crystal structure of jadeite,  $NaAlSi_3O_6$ . *Amer. Mineralogist* **51**, 956–975.
- E. W. RADOSLOVICH (1960), The structure of muscovite,  $KAl_2(Si_3Al)O_{10}(OH)_2$ . *Acta Crystallogr.* **13**, 919–932.
- M. ROSS, H. TAKEDA and D. R. WONES (1966), Mica polytypes: systematic description and identification. *Science* **151**, 191–193.
- R. SADANAGA and Y. TAKÉUCHI (1961), Polysynthetic twinning of micas. *Z. Kristallogr.* **116**, 406–429.
- W. G. SLY, D. P. SHOEMAKER and J. H. VAN DEN HENDE (1962), Two- and three-dimensional crystallographic Fourier summation program for the IBM 7090 computer. Esso Research and Engineering Co., Central Basic Research Laboratory.

- J. V. SMITH and S. W. BAILEY (1963), Second review of Al—O and Si—O tetrahedral distances. *Acta Crystallogr.* **16**, 801—811.
- J. V. SMITH and H. S. YODER, JR. (1956), Experimental and theoretical studies of the mica polymorphs. *Mineral. Mag.* **31**, 209—231.
- H. STEINFINK (1962), Crystal structure of a trioctahedral mica: phlogopite. *Amer. Mineralogist* **47**, 886—896.
- Y. TAKÉUCHI (1966), Structures of brittle micas. *Proc. Thirteenth Nat. Conf. on Clays and Clay Minerals*, Pergamon Press, p. 1—24.
- B. VELDE (1965), Experimental determination of muscovite polymorphs. *Amer. Mineralogist* **50**, 436—449.
- A. R. VERMA and P. KRISHNA (1966), Polymorphism and polytypism in crystals. Chapters 1 and 4. John Wiley and Sons, New York.
- H. S. YODER, JR., and H. P. EUGSTER (1955), Synthetic and natural muscovites. *Geochim. Cosmochim. Acta* [London] **8**, 225—280.
- B. B. ZVYAGIN (1962), A theory of polymorphism of micas. *Soviet Physics—Crystallography*, **6**, 571—580 (in translation).